

# UCLA

## UCLA Previously Published Works

### Title

Charge Density in Enzyme Active Site as a Descriptor of Electrostatic Preorganization

### Permalink

<https://escholarship.org/uc/item/7c97g43d>

### Journal

Journal of Chemical Information and Modeling, 59(5)

### ISSN

1549-9596

### Authors

Fuller, Jack  
Wilson, Tim R  
Eberhart, Mark E  
[et al.](#)

### Publication Date

2019-05-28

### DOI

10.1021/acs.jcim.8b00958

Peer reviewed

# Charge Density in Enzyme Active Site as a Descriptor of Electrostatic Preorganization

Jack Fuller III,<sup>1</sup> Tim R. Wilson,<sup>2</sup> Mark E. Eberhart,<sup>2</sup> and Anastassia N. Alexandrova<sup>1,3,\*</sup>

<sup>1</sup>*Department of Chemistry and Biochemistry, University of California, Los Angeles, Los Angeles, CA, 90095, USA*

<sup>2</sup>*Molecular Theory Group, Colorado School of Mines, USA*

<sup>3</sup>*California NanoSystems Institute, Los Angeles, CA, 90095, USA*

Corresponding Author e-mail: [ana@chem.ucla.edu](mailto:ana@chem.ucla.edu)

**RECEIVED DATE:** XX XX 2018

**ABSTRACT:** Large protein macromolecules in enzymatic catalysis have been shown to exert a specific electric field that reduces the reorganization energy upon barrier crossing and thus reduces the reaction free energy barrier. In this work we suggest that the charge density in the active site of an enzyme investigated using formalisms embodied by the quantum theory of atoms in molecules (QTAIM) provides a sensitive and quantum mechanically rigorous probe of electrostatic preorganization. We focus on the active site of ketosteroid isomerase, a well-studied enzyme for which electrostatic preorganization has been modeled theoretically and studied experimentally. We study the charge density in the active site, and the reaction mechanism in the presence of small external electric fields of various directions and magnitudes. We show that the geometry of the full charge density is a sensitive reporter on the external field experienced by the active site. Changes are observed in the relative positions of critical points and amount of charge at critical points as a function of the field. At the same time, a subset of these features correlates linearly with the barrier of the first reaction step in catalysis. Small changes in the barrier, within 1-2 kcal/mol, are reflected in the charge density, suggesting the existence of a

field - reactant state charge density - reaction barrier correlation. Hence, QTAIM can be used for the analysis of electric field in enzyme active sites, and further investigations and exploitations of the found correlations may prove useful in enzyme design where preorganization is optimized.

## **INTRODUCTION**

Nature developed large protein macromolecules to host enzyme active sites. While part of the macromolecules' role is to shield the active site from the cell environment, it does not necessarily justify their sizes, structural complexity, and diversity. As a way to account for these large protein scaffolds it was hypothesized and recently confirmed: the charged groups in the protein create an electric field preorganized to favor the rate-limiting transition state (TS) of the catalytic reaction. This phenomenon, called electrostatic preorganization, was introduced in 1998 by Warshel.<sup>1,2</sup> Non-enzymatic reactions occurring in solvents are accompanied by solvent reorganization, which lowers the enthalpy of the TS. However, there is an entropic penalty for solvent reorganization. Thanks to the enzymes' electrostatic environment, which minimizes transition state energies relative to those of the reactants, enzymatic catalytic reactions pay no such entropic penalty, and thus have overall lower free energy barriers. It was additionally shown by several groups<sup>3</sup> that the majority of this effect, expectedly, is rather short-range and comes mainly from the first and second coordination sphere residues. It is therefore a role of the protein macromolecule to position those amino acids in just the right orientation so that the field produced will align with the charge redistribution along the reaction coordinate.

Electrostatic preorganization can be probed experimentally using time-resolved fluorescence and vibrational Stark spectroscopy.<sup>4-6</sup> In 2014, Boxer

investigated the preorganization by probing local electric field in ketosteroid isomerase (KSI), which was also the example protein studied by Warshel. KSI is well-studied with an extremely high unimolecular rate constant, making it an ideal candidate for computational studies. KSI forms a charged enolate intermediate possessing a polar carbonyl. The ability of the enzyme to stabilize this enolate is a key feature of its remarkable catalytic efficiency. Boxer showed that the electric field acting on the carbonyl of the substrate (or bound inhibitor) is directly correlated to the free energy barrier of the reaction, with the slope corresponding to the change in dipole moment of the carbonyl between the reactant state and transition state.<sup>5,6</sup>

In addition to these experimental studies, significant theoretical efforts have computationally examined the origins, magnitude, and consequences of electrostatic preorganization. Warshel evaluated the effect of preorganization through the empirical valence bond (EVB) method, which probes the changes in the contributions of different resonance forms to the TS.<sup>7,8</sup> Hammes-Schiffer and co-workers have verified Boxer's results on KSI using computational vibrational probes.<sup>9</sup> They also used thiocyanite probes to track changes to the active site electrostatic environment of dihydrofolate reductase, which undergoes large conformational changes during the reaction.<sup>10</sup> The protein conformational rearrangements were shown to induce changes in the electrostatic interactions between the probes and their surroundings. Furthermore, contributions to the electric field of the active site from individual residues throughout the protein were identified computationally, and this information may be used to identify mutations that could affect the electric field and hence the catalytic rate. Head-Gordon's group used a polarizable force field to detect the fields and also proposed mutations in the second coordination sphere which they suggested would improve the activity of artificial enzymes catalyzing Kemp elimination.<sup>11,12</sup>

Several theoretical and even experimental works demonstrated that charge density,  $\rho$ , in the active site can report on protein electrostatics.<sup>13-23</sup> Quantum topological analyses via QTAIM and ELF as well as experimental

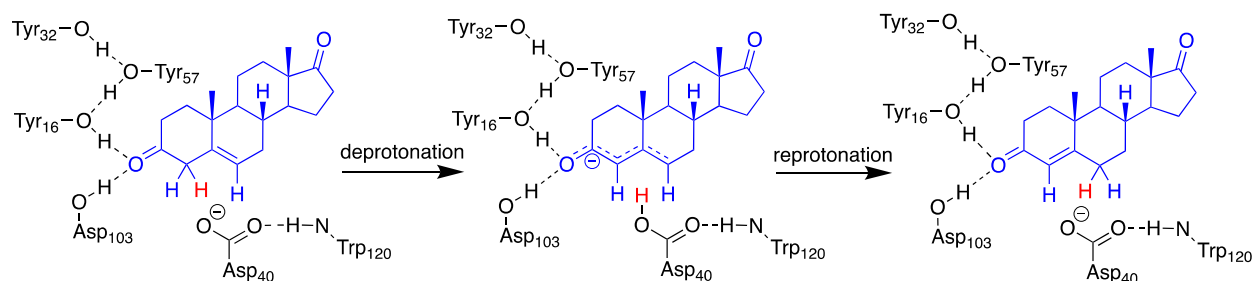
ways to access  $\rho$  have been used to gain insight into enzyme functionality and inhibition.<sup>21,22</sup> In our enzyme redesign study focusing on carboxypeptidase A (CPA), we uncovered a relationship between the  $\rho$  of enzyme-substrate reactant complexes and the first reaction step's free energy of activation.<sup>24</sup> Moreover, we recently demonstrated that electrostatic preorganization could be probed via charge density critical point (CP) analysis.<sup>25</sup> Using HDAC8 as a test case,<sup>25,26</sup> we showed that the positions of active site CPs in  $\rho$  are perturbed by the protein's extended environment, especially by the polar or charged groups. The distances between CPs and the curvature of the charge density at these points have been related to the vibrational frequency along the reaction coordinates through the electron preceding perspective proposed by Ayers and co-workers.<sup>27,28</sup> Bader's application of catastrophe theory to chemical reactions implies that mechanisms may be described solely in terms of relative CP positions.<sup>29</sup> Jones et al. have demonstrated the applicability of this approach by using the distance between CPs as an order parameter for structural phase transformations.<sup>30</sup>

Here, we advance the argument that it may be possible to extract barrier information directly from  $\rho$  by demonstrating that features of the charge density in the chemically relevant parts of a reaction complex under the effect of the external field are indicative of the reaction barrier's magnitude.

The system that we interrogate is KSI, for which a wealth of experimental and theoretical data is available. In order to decouple the sole effect of the field from the possible conformational and dynamical changes in the protein upon the change of its sequence, we apply external, well-defined, and uniform fields of different magnitudes. From our findings, we propose that  $\rho$  in the active site with the bound substrate (or rate-determining intermediate) emerges as a feasible quantum mechanical descriptor of electrostatic preorganization.

## METHODS

Previous mechanistic studies as well as works by Boxer and Markland<sup>3</sup> demonstrated that the majority of the field that affects the reaction mechanism and barrier in KSI comes from the residues in the immediate vicinity of the substrate. This informed our choice of the active site considered explicitly (included residues are shown in Scheme 1 and Figure 1). These residues comprise the catalytic base and the residues forming the hydrogen bond network around the substrate and catalytic base. The specific electronic effects of these hydrogen bonds are important for catalysis and cannot be modeled with a uniform external electric field, so they were modeled explicitly. The starting structure of KSI with the bound substrate was built based on the crystal structure (PDB code 1OH0).<sup>31</sup> Scheme 1 depicts the proposed reaction mechanism while Figure 1 shows the positioning of the active site within the full protein. The attachment points through which the ligands of Scheme 1 connect to the rest of the protein were fixed to the positions defined by the rest of the protein. For the purpose of our model, the rest of the protein was deleted.



**Scheme 1.** Schematic representation of the active site of KSI and the reaction mechanism. Residues shown in this Scheme were included explicitly in the present study.

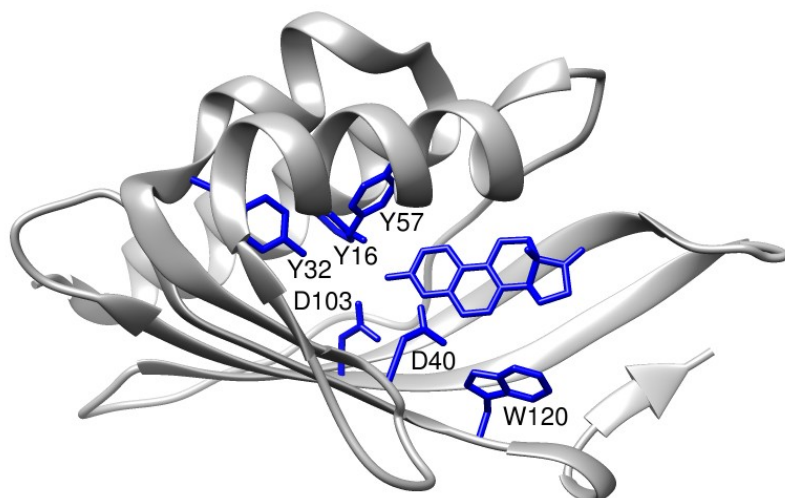


**Figure 1.** The full KSI protein with the region selected for this study shown in blue.

This model was used for the mechanistic study with and without an applied electric field. All calculations were done with Turbomole,<sup>32-42</sup> employing the M06-2X density functional.<sup>43</sup> The def2-SVP basis set was used for geometry optimizations, and the def2-TZVP basis set was used for electronic energies.<sup>44</sup> Solvation was modeled with COSMO<sup>45</sup> with the dielectric constant set to 4, which is typical for studies of buried enzyme active sites.<sup>46</sup>

Other studies, as well as our own, based on the classical AMBER charges and truncated multiple expansion, predict that the protein beyond the active site produces a field on the order of 10 MV/cm, i.e., roughly an order of magnitude lower than the field produced by the first and second coordination sphere residues. Hence, in this work, we will apply the highly-controlled, uniform, external electric fields to the active site of KSI shown in Figure 2. Specifically, the selected directions of the field are along the C=O bond (with the positive direction defined as C to O), along the vector connecting the carbonyl oxygen and the  $\alpha$ -carbon being deprotonated, and along the vector connecting the carbonyl oxygen and the oxygen of the catalytic base. The active site was optimized at every stationary point along

the reaction profile with each applied field, subject to constraints imposed by the attachments to the protein macrostructure. The nature of the stationary points was confirmed by frequency calculations: zero imaginary frequencies for the reaction intermediates and one imaginary frequency for the transition states (TSs). The majority of the field at the active site originate from the residues modeled explicitly, and hence the electronic structure calculations implicitly include this field as well as local chemical bonding and geometric effects. The effect of the rest of the protein is subtler, and it is not obvious that our usual methods would have the sensitivity and rigor to account for the fields of smaller magnitudes produced by the protein. We investigate the extent to which the topological and geometric structure of  $\rho$  can be used as such a probe. For the present development and calibration of the method, the simple and uniform field was essential; if in contrast the field variations are achieved through mutations to the protein sequence, the protein structure and dynamics responds, many charged groups move, and that may affect not only the field in the active site but also its structure. Hence, the isolated effect of the field on the reaction barrier will not be easily extracted. Our model targets the isolated effect of the field, since our goal is to use the geometry of  $\rho$  specifically to detect the field and electrostatic preorganization.

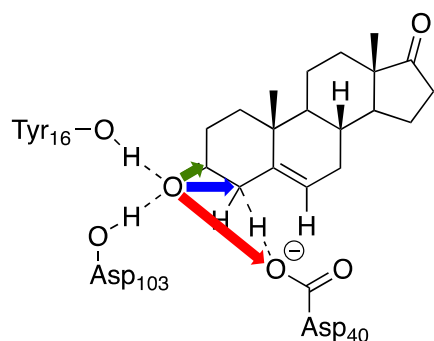


**Figure 2.** Selected directions of the applied electric field in this study.



The QTAIM formalism was used to analyze the charge density in the active site model of KSI in the presence of the mentioned external fields. The density used in the QTAIM analysis was produced by DFT calculations in the reactant state with the calculation settings described above. The features in the charge density that were scrutinized as a first approximation to charge density geometry include the bond CPs' charge densities, and their locations. The analysis focused on the bond CPs relevant to the catalytic mechanism: the activated carbonyl, the network of hydrogen bonds participating in the carbonyl activation, and the network of hydrogen bonds that includes the Asp-40 residue, which participates in the deprotonation/reprotonation events in the two reaction steps (Figure 3).

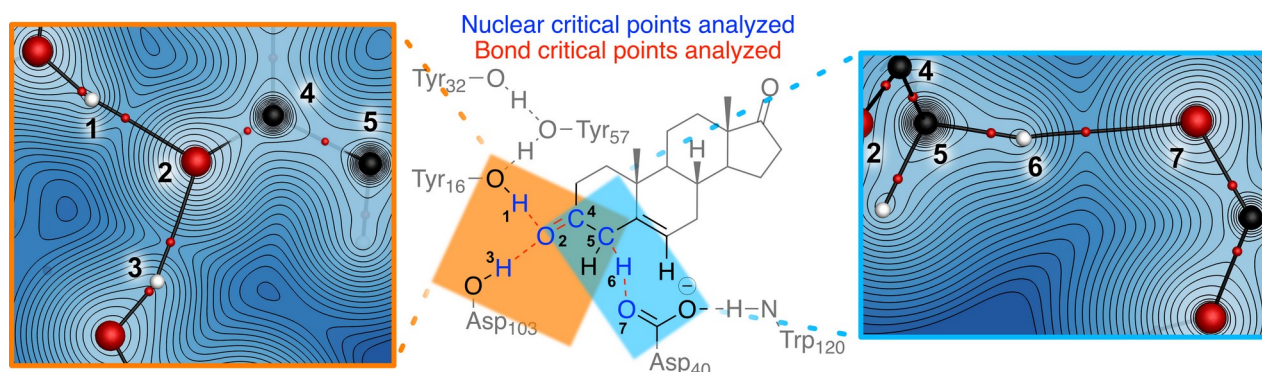


**Figure 3.** The objects in  $\rho$  analyzed by QTAIM in this work: (center) schematic representation, (sides) actual typical plot of the charge density built using the DFT density in this study; the orange and cyan rectangles in the center diagram indicate the regions shown in the panels. The orange rectangle corresponds to the cut plane defined by atoms (1,2,3) and the cyan to the plane defined by atoms (5,6,7). Bond CPs are shown in as small red dots.

## RESULTS AND DISCUSSION

Figure 4A shows the calculated reaction profile for the mechanism of Scheme 1 with varying applied field. The reaction profile derived from the experiment is also shown for comparison. The field of -10 MV/cm (in the O to

C direction along the carbonyl bond) favors the activation of the carbonyl group by pushing the electrons toward its O atom. As a result, the first step of the reaction is facilitated and the barrier is reduced by 2.1 kcal/mol compared to the reaction profile calculated without the applied electric field. However, the following enolate intermediate is stabilized even more, by 5.4 kcal/mol. In the second reaction step, consisting of the reprotonation of the substrate, the electron movement in the area of the activated carbonyl is opposite to that in the first reaction step. Hence, with the -10 MV/cm external field, this step becomes slower: the barrier increases by 3.5 kcal/mol. With the +10 MV/cm field applied opposing the carbonyl activation, the situation is reversed, and the first barrier grows by 1.8 kcal/mol. The enolate intermediate is accordingly destabilized by 5.8 kcal/mol and the second barrier drops by 2 kcal/mol. The changes found in the reaction energetics should not be taken as suggestions for altering enzyme performance through an applied field, because our fields are uniform and thus unphysical. In reality, the heterogeneity of the protein structure would produce more complicated fields and more complicated effects on the reaction profile. Notice, also, that the zero field reaction profile is the closest to experiment,<sup>47</sup> in-line with the fact that the majority of the electric field required to facilitate the reaction comes from the residues in the immediate proximity,<sup>3</sup> i.e., the ones explicitly included in the model. Relatively small changes in the reaction energetics and no change of mechanism are the desirable effects for the purposes of this work so we can analyze the sensitivity and rigor of our approach in probing the field effects in isolation from other factors.

Depicted in Figure 4B are the barriers for the two reaction steps as functions of the applied external field. Both barriers show near perfect linear correlations. The slopes of the lines are opposite, as expected, since different directions of the field favor different reaction steps. Hence, reaction kinetics readily and predictably respond to the external field.

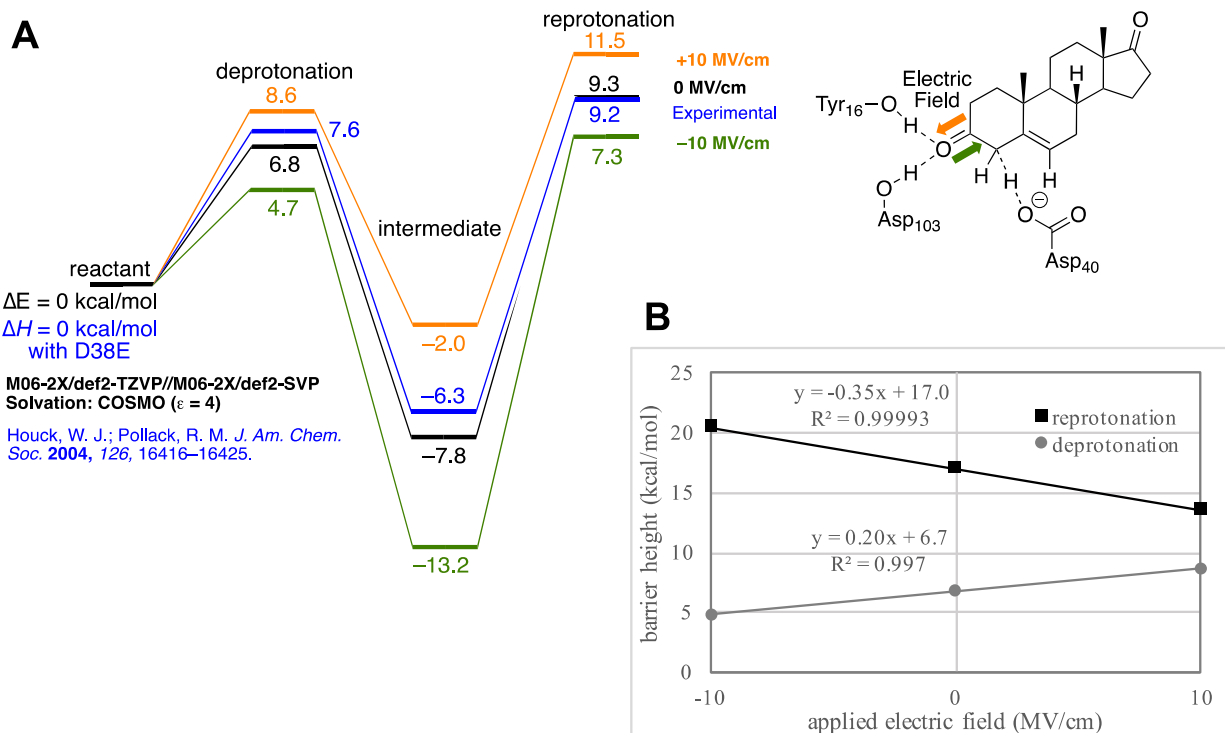


**Figure 4.** (A) KSI reaction profiles from experiment (blue, from ref. 45) and calculations with varying applied external fields: +10 MV/cm (yellow), -10 MV/cm (green), and zero field (black). The directions of the field with respect to the active site are shown in the inset for clarity. (B) Correlations of the computed barriers for the two steps of the reaction with the applied electric fields.

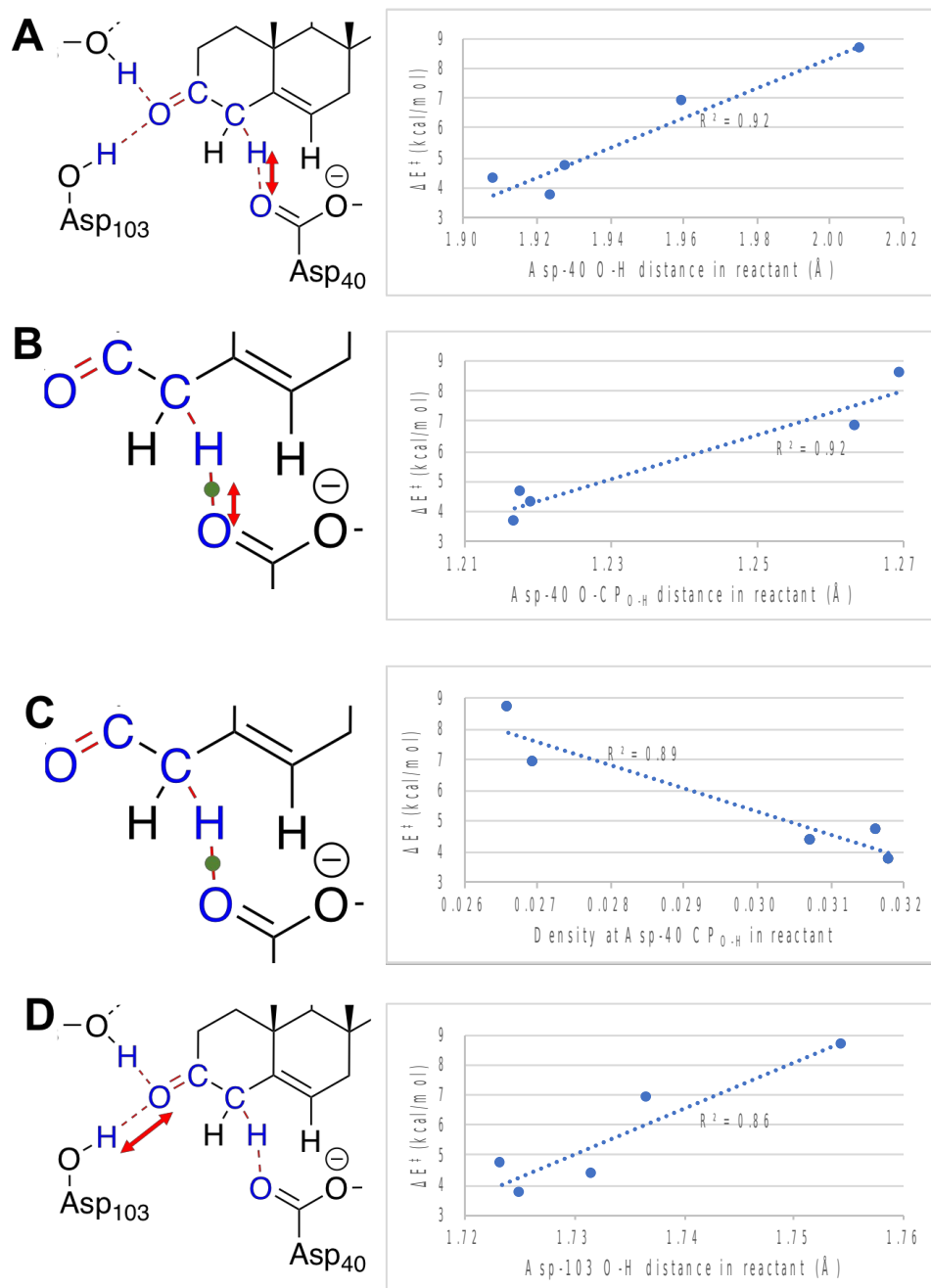


**Figure 5.** Geometric and QTAIM parameters found to exhibit the best correlations with the computed reaction barriers for the first step of the reaction at varying external electric fields: (A) the Asp-40 O-H distance, (B) the distance between the Asp-40 CP<sub>O-H</sub> and the Asp-40 O atom, (C) the charge density at the Asp-40 CP<sub>O-H</sub>, and (D) the Asp-103 O-H distance.

**Table 1.** Computed correlations between reactant properties and barrier heights.

<b>Property</b>	<b>R<sup>2</sup> (vs. <math>\Delta E^\ddagger</math>)</b>
Asp-40 O-H distance (Å)	0.92490
Asp-40 O-CP <sub>O-H</sub> distance (Å)	0.92044
density at Asp-40 CP <sub>O-H</sub>	0.89403
Asp-103 O-H distance (Å)	0.85884
Tyr-16 O-H distance (Å)	0.81701
Asp-40 H-CP <sub>O-H</sub> distance (Å)	0.49461
density at Tyr-16 CP <sub>O-H</sub>	0.24130
density at Asp-103 CP <sub>O-H</sub>	0.20801
Asp-103 O-CP <sub>O-H</sub> distance (Å)	0.19741
C-CP <sub>C=O</sub> distance (Å)	0.07380
Tyr-16 O-CP <sub>O-H</sub> distance (Å)	0.03876
C-CP <sub>C-H</sub> distance (Å)	0.01902
O-CP <sub>C=O</sub> distance (Å)	0.00392
density difference (CP <sub>C-H</sub> - CP <sub>O-H</sub> )	0.00376
H-CP <sub>C-H</sub> distance (Å)	0.00104
density at CP <sub>C=O</sub>	0.00006
density at CP <sub>C-H</sub>	0.00002

Next we investigated the extent to which features of  $\rho$  in the active site of the reactant state (i) respond to the applied field and (ii) are indicative of the subsequent reaction energetics. In Figure 5 and Table 1 we show correlations between several active site CPs characteristic subjected to applied external fields, and the corresponding reaction barriers. Surprisingly, the investigated characteristics of the activated carbonyl group do not exhibit the strongest correlations. Instead, the best correlations are found in the area of coordination to Asp40, where the reaction takes place.

Our findings indicate that CP characteristics of the charge density in the reactant state of the active site correlate nicely with the reaction barrier. At the same time, the barrier correlates linearly with the applied electric field across its full range. We also note that the features that best reflect the electric field originating outside of the active site are the CPs of the oxygen-hydrogen bonds. Notice that the geometry of the active site CPs is capable of differentiating between electronic structures of the active site that produce very small changes to the reaction barriers, on the order of 1–3 kcal/mol. This sensitivity is remarkable, especially considering that the charge density is analyzed in the reactant state. Accordingly, we hypothesize a  $\rho$ -field-activity correlation, and conclude that CP analysis may serve as a sensitive probe for electrostatic preorganization.

Even so, simple CP analysis has its limitations. For one thing, the applied field causes the overall charge redistribution, and not just the change of charge in the CPs. Because  $\rho$  is a continuous smooth function, changes in one region necessarily affects  $\rho$  at other active site locations. It is likely that nature produces optimized charge densities with finely tuned heterogeneous electrostatic fields that exploit such correlations. The overall charge redistribution is controlled by the Ehrenfest force from the electrostatic field, which acts on surfaces of zero flux (ZFS) in the gradient of the charge density, surfaces that contain the CPs. Effectively, CPs are tethered together by these surfaces.<sup>48</sup> Hence the correlated response of the charge density to an electrostatic field may be investigated by observing the motion of the ZFS due to an electrostatic field. In our preliminary work addressing this type of motion, we find that cage CPs (local minima of  $\rho$ ) play a consequential role in charge redistribution. We will discuss these finding in more detail in a subsequent paper.

In this paper we address only electronic energy rather than free energy barriers to the reaction. It is an approximation since the theory of electrostatic preorganization concerns free energy barriers. However, it is important to recognize that the protein is preorganized in the sense that the

field that it exerts is optimal for the reaction. Therefore, the entropic penalty to reorganize the environment upon crossing the reaction barrier will be minimal. Still, the field itself can affect only the enthalpic barrier to the reaction, while entropic contributions will be minimized if the system evolves through the reaction into configurations providing optimal fields. Also, because enthalpy and entropy correlate, it is reasonable to consider the effects of the field on the reaction enthalpy and probe the effects with the QTAIM formalism. Later the entropic effect can be addressed separately through molecular dynamics.

## **CONCLUSIONS**

Electrostatic preorganization - the effect of the specific electric field exerted by the protein macromolecule on the active site, and favoring the catalyzed reaction - needs to be understood, accurately captured in theory and experiment, and eventually designed in artificial enzymes. We demonstrate that geometric features of the enzyme active site charge density serve as quantum mechanically rigorous probes of electrostatic preorganization. The exemplar explored in this work is the KSI enzyme, modeled as an isolated large cluster representing the active site, in the presence of small, well-defined external electric fields of varying directions. The charge density of the KSI active site calculated at the DFT level sensitively responds to the subtle changes in the external electric field, and at the same time reports on (and predicts) the reaction barrier. We note the uniform field is a necessary feature of the model, ensuring that the captured changes in the QTAIM features of the active site are due solely to the changing field. In a real protein system, the field is heterogeneous. Firstly, this would mean that every CP studied in this work would experience very different fields due to the protein heterogeneity. Secondly, any changes in protein macromolecule would induce both the complex changes in the local electric fields, and the subtle structural changes in the active site that in turn would induce additional field changes. Given such a convoluted picture, it

would hard to deconvolute the QTAIM signal. Hence, in this study, the simple model was required to validate QTAIM as a rigorous and sensitive reporter on the fields and the resultant changes in the reaction barriers. The features in  $\rho$  that both respond to the field, and correlate with the reaction newbarrier are the ones involved in the KSI catalyzed reaction. The best correlations are found for the objects in  $\rho$  at the contact of the substrate with Asp40, the residue directly participating in the proton abstraction and reprotonation, in the first and second reaction steps, respectively. We find nearly perfect field-density-barrier correlations, with the field-induced differences in reaction barriers on the order of 1-2 kcal/mol faithfully detected/predicted by CP analysis.

We note the uniform field is a necessary feature of the model, ensuring that the captured changes to the active site CPs were attributable only the changing field. However, we note that real proteins certainly optimize electrostatic preorganization via heterogeneous fields that exploit correlated charge redistribution around separated CPs. Also, any changes in a real protein macromolecule would induce both the complex changes in the local electric fields, and the subtle structural changes in the active site that in turn would induce additional field changes, making the signal detected by QTAIM highly convoluted. Hence, in this study, the simple model was required to validate QTAIM as a rigorous and sensitive reporter on the fields and the resultant changes in the reaction barriers. However, we propose a further refinement to the method employed here that would permit a more detailed description of such correlated charge redistribution induced by electrostatic preorganization. The correlated feature space of  $\rho$  could eventually be used in sequence engineering and enzyme design that includes electrostatic preorganization as a parameter.

**Supporting Information.** M06-2X/def2-TZVP//M06-2X/def2-SVP COSMO( $\epsilon = 4$ ) - Solvated Electronic Energies (Hartrees) and Cartesian Coordinates (Bohr).



**Acknowledgements:** Financial support comes from the NSF-CAREER Award CHE-1351968 to A.N.A.. We also acknowledge the UCLA-IDRE cluster Hoffman2 for computational resources.

## References:

1. Warshel, A. Electrostatic Origin of the Catalytic Power of Enzymes and the Role of Preorganized Active Sites. *J. Biol. Chem.* **1998**, *273*, 27035-27038.
2. Warshel, A.; Sharma, P. K.; Kato, M.; Xiang, Y.; Liu, H.; Olsson, M. H. M. Electrostatic Basis for Enzyme Catalysis. *Chem. Rev.* **2006**, *106*, 3210-3235.
3. Wang, L.; Fried, S. D.; Markland, T. E. Proton Network Flexibility Enables Robustness and Large Electric Fields in the Ketosteroid Isomerase Active Site. *J. Phys. Chem. B* **2017**, *121*, 9807-9815.
4. Childs, W.; Boxer, S. G. Solvation Response along the Reaction Coordinate in the Active Site of Ketosteroid Isomerase. *J. Am. Chem. Soc.* **2010**, *132*, 6474-6480.
5. Fried, S. D.; Bagchi, S.; Boxer, S. G. Extreme Electric Fields Power Catalysis in the Active Site of Ketosteroid Isomerase. *Science* **2014**, *346*, 1510-1514.
6. Wu, Y.; Boxer, S. G. A Critical Test of the Electrostatic Contribution to Catalysis with Noncanonical Amino Acids in Ketosteroid Isomerase. *J. Am. Chem. Soc.* **2016**, *138*, 11890-11895.
7. Warshel, A.; Sharma, P. K.; Chu, Z. T.; Åqvist, J. Electrostatic Contributions to Binding of Transition State Analogues Can Be Very Different from the Corresponding Contributions to Catalysis: Phenolates Binding to the Oxyanion Hole of Ketosteroid Isomerase. *Biochemistry* **2007**, *46*, 1466-1476.
8. Kamerlin, S. C. L.; Sharma, P. K.; Chu, Z. T.; Warshel, A. Ketosteroid Isomerase Provides Further Support for the Idea that Enzymes Work by Electrostatic Preorganization. *Proc. Natl. Acad. Sci. U. S. A.* **2010**, *107*, 4075-4080.
9. Layfield, J. P.; Hammes-Schiffer, S. Calculation of Vibrational Shifts of Nitrile Probes in the Active Site of Ketosteroid Isomerase upon Ligand Binding. *J. Am. Chem. Soc.* **2013**, *135*, 717-725.
10. Liu, C. T.; Layfield, J. P.; Stewart, R. J., III; French, J. B.; Hanoian, P.; Asbury, J. B.; Hammes-Schiffer, S.; Benkovic, S. J. Probing the Electrostatics of Active Site Microenvironments along the Catalytic Cycle for *Escherichia coli* Dihydrofolate Reductase. *J. Am. Chem. Soc.* **2014**, *136*, 10349-10360.
11. Bhowmick, A.; Sharma, S. C.; Head-Gordon, T. The Importance of the Scaffold for *de Novo* Enzymes: A Case Study with Kemp Eliminase. *J.*

- Am. Chem. Soc.* **2017**, *139*, 5793–5800.
12. Vaissier, V.; Sharma, S. C.; Schaettle, K.; Zhang, T.; Head-Gordon, T. Computational Optimization of Electric Fields for Improving Catalysis of a Designed Kemp Eliminase. *ACS Catal.* **2018**, *8*, 219–227.
  13. Franzen, S.; Goldstein, R. F.; Boxer, S. G. Electric Field Modulation of Electron Transfer Reaction Rates in Isotropic Systems: Long Distance Charge Recombination in Photosynthetic Reaction Centers. *J. Phys. Chem.* **1990**, *94*, 5135–5149.
  14. Gopher, A.; Blatt, Y.; Schonfeld, M.; Okamura, M. Y.; Feher, G.; Montal, M. The Effect of an Applied Electric Field on the Charge Recombination Kinetics in Reaction Centers Reconstituted in Planar Lipid Bilayers. *Biophys. J.* **1985**, *48*, 311–320.
  15. Popovic, Z. D.; Kovacs, G. J.; Vincett, P. S.; Alegria, G.; Dutton, P. L. Electric Field Dependence of Recombination Kinetics in Reaction Centers of Photosynthetic Bacteria. *Chem. Phys.* **1986**, *110*, 227–237.
  16. Lehle, H.; Kriegl, J. M.; Neienhaus, K.; Deng, P.; Fengler, S.; Nienhaus, G. U. Probing Electric Fields in Protein Cavities by Using the Vibrational Stark Effect of Carbon Monoxide. *Biophys. J.* **2005**, *88*, 1978–1990.
  17. Wang, X.; He, X.; Zhang, J. Z. H. Predicting Mutation-Induced Stark Shifts in the Active Site of a Protein with a Polarized Force Field. *J. Phys. Chem. A* **2013**, *117*, 6015–6023.
  18. Sowlati-Hashjin, S.; Matta, C. F. The Chemical Bond in External Electric Fields: Energies, Geometries, and Vibrational Stark Shifts of Diatomic Molecules. *J. Chem. Phys.* **2013**, *139*, No. 144101.
  19. Shaik, S.; de Visser, S. P.; Kumar, D. External Electric Field Will Control the Selectivity of Enzymatic-Like Bond Activations *J. Am. Chem. Soc.* **2004**, *126*, 11746–11749.
  20. Matta, C. F. Modeling Biophysical and Biological Properties from the Characteristics of the Molecular Electron Density, Electron Localization and Delocalization Matrices, and the Electrostatic Potential. *J. Comp. Chem.* **2014**, *35*, 1165–1198 and references therein.
  21. Arabi, A. A.; Matta, C. F. Effects of External Electric Fields on Double Proton Transfer Kinetics in the Formic Acid Dimer. *Phys. Chem. Chem. Phys.* **2011**, *13*, 13738–13748.
  22. Fang, D.; Lord, R. L.; Cisneros, G. A. Ab Initio QM/MM Calculations Show an Intersystem Crossing in the Hydrogen Abstraction Step in Dealkylation Catalyzed by AlkB *J. Phys. Chem. B* **2013**, *117*, 6410–6420.
  23. Lohrman, J.; Vazquez-Montelongo, E. A.; Pramanik, S.; Day, V. W.; Hix, M. A.; Bowman-James, K.; Cisneros, G. A. Characterizing Hydrogen-Bond Interactions in Pyrazinetetracarboxamide Complexes: Insights from Experimental and Quantum Topological Analyses. *Inorg. Chem.* **2018**, *57*, 9775–9778.

24. Valdez, C. E.; Morgenstern, A.; Eberhart, M. E.; Alexandrova, A. N. Predictive Methods for Computational Metalloenzyme Redesign – a Test Case with Carboxypeptidase A. *Phys. Chem. Chem. Phys.* **2016**, *18*, 31744–31756.
25. Morgenstern, A.; Jaszai, M.; Eberhart, M. E.; Alexandrova, A. N. Quantified Electrostatic Preorganization in Enzymes Using the Geometry of the Electron Charge Density. *Chem. Sci.* **2017**, *8*, 5010–5018.
26. Nechay, M. R.; Gallup, N. M.; Morgenstern, A.; Smith, Q. A.; Eberhart, M. E.; Alexandrova, A. N. Histone Deacetylase 8: Characterization of Physiological Divalent Metal Catalysis. *J. Phys. Chem. B* **2016**, *120*, 5884–5895.
27. Ayers, P. W.; Jenkins, S. An Electron-Preceding Perspective on the Deformation of Materials. *J. Chem. Phys.* **2009**, *130*, No. 154104.
28. Guevara-García, A.; Echegaray, E.; Toro-Labbe, A.; Jenkins, S.; Kirk, S. R.; Ayers, P. W. Pointing the Way to the Products? Comparison of the Stress Tensor and the Second- Derivative Tensor of the Electron Density. *J. Chem. Phys.* **2011**, *134*, No. 234106.
29. Bader, R. F. W., *Atoms in Molecules. A Quantum Theory* (Clarendon Press, Oxford, UK, 1990).
30. Jones, T.E., Eberhart M.E., Clougherty, D.P., Topological Catastrophe and Isostructural Phase Transition in Calcium. *Phys. Rev. Lett.* **2010**, *105*, 265702.
31. Kim, S. W.; Cha, S.-S.; Cho, H.-S.; Kim, J.-S.; Ha, N.-C.; Cho, M.-J.; Joo, S.; Kim, K. K.; Choi, K. Y.; Oh, B.-H. High-Resolution Crystal Structures of  $\Delta^5$ -3-Ketosteroid Isomerase with and without a Reaction Intermediate Analogue. *Biochemistry* **1997**, *36*, 14030–14036.
32. Ahlrichs, R.; Bär, M.; Häser, M.; Horn, H.; Kölmel, C. Electronic Structure Calculations on Workstation Computers: The Program System TURBOMOLE. *Chem. Phys. Letters* **1989**, *162*, 165–169.
33. Häser, M.; Ahlrichs, R. Improvements on the Direct SCF Method. *J. Comput. Chem.* **1989**, *10*, 104–111.
34. Treutler, O.; Ahlrichs, R. Efficient Molecular Numerical Integration Schemes. *J. Chem. Phys.* **1995**, *102*, 346–354.
35. Eichkorn, K.; Weigend, F.; Treutler, O.; Ahlrichs, R. Auxiliary Basis Sets for Main Row Atoms and Transition Metals and Their Use to Approximate Coulomb Potentials. *Theor. Chem. Acc.* **1997**, *97*, 119–124.
36. Eichkorn, K.; Treutler, O.; Öhm, H.; Häser, M.; Ahlrichs, R. Auxiliary Basis Sets to Approximate Coulomb Potentials. *Chem. Phys. Letters* **1995**, *242*, 652–660.
37. Weigend, F. Accurate Coulomb-Fitting Basis Sets for H to Rn. *Phys. Chem. Chem. Phys.* **2006**, *8*, 1057–1065.
38. Sierka, M.; Hogekamp, A.; Ahlrichs, R. Fast Evaluation of the Coulomb Potential for Electron Densities Using Multipole Accelerated Resolution of Identity Approximation. *J. Chem. Phys.* **2003**, *118*,

- 9136-9148.
39. Deglmann, P.; May, K.; Furche, F.; Ahlrichs, R. Nuclear Second Analytical Derivative Calculations Using Auxiliary Basis Set Expansion. *Chem. Phys. Letters* **2004**, *384*, 103-107.
  40. Arnim, M. v.; Ahlrichs, R. Parallelization of Density Functional and RI-Coulomb Approximation in Turbomole. *J. Comp. Chem.* **1998**, *19*, 1746-1757.
  41. Arnim, M. v.; Ahlrichs, R. Geometry Optimization in Generalized Natural Internal Coordinates. *J. Chem. Phys.* **1999**, *111*, 9183-9190.
  42. Ahlrichs, R. Efficient Evaluation of Three-Center Two-Electron Integrals Over Gaussian Functions. *Phys. Chem. Chem. Phys.* **2004**, *6*, 5119-5121.
  43. Zhao, Y.; Truhlar, D. G. The M06 Suite of Density Functionals for Main Group Thermochemistry, Thermochemical Kinetics, Noncovalent Interactions, Excited States, and Transition Elements: Two New Functionals and Systematic Testing of Four M06-Class Functionals and 12 Other Functionals. *Theor. Chem. Acc.* **2008**, *120*, 215-241.
  44. Weigend, F.; Ahlrichs, R. Balanced Basis Sets of Split Valence, Triple Zeta Valence and Quadruple Zeta Valence Quality for H to Rn: Design and Assessment of Accuracy. *Phys. Chem. Chem. Phys.* **2005**, *7*, 3297-3305.
  45. Klamt, A.; Schüürmann, G. COSMO: A New Approach to Dielectric Screening in Solvents with Explicit Expressions for the Screening Energy and its Gradient. *J. Chem. Soc., Perkin Trans. 2* **1993**, No. 5, 799-805.
  46. Sahakyan, A. B. Computational Studies of Dielectric Permittivity Effects on Chemical Shifts of Alanine Dipeptide. *Chem. Phys. Lett.* **2012**, *547*, 66-72.
  47. Houck, W. J.; Pollack, R. M. Temperature Effects on the Catalytic Activity of the D38E Mutant of 3-Oxo- $\Delta^5$ -Steroid Isomerase: Favorable Enthalpies and Entropies of Activation Relative to the Nonenzymatic Reaction Catalyzed by Acetate Ion. *J. Am. Chem. Soc.* **2004**, *126*, 16416-16425.
  48. Morgenstern, A., Morgenstern, C., Miorelli, J., Wilson, T., Eberhart, M.E. The Influence of Zero-Flux Surface Motion on Chemical Reactivity. *Phys. Chem. Chem. Phys.* **2016**, *91*, 5638-5646.

## TOC Graphics:

